Large scale hydraulic conductivity of the soil deposits of the Venezia Lagoon from numerical back-analysis

E. Giacomini, F. Colleselli & F. Cattaneo
Università degli Studi di Brescia, Brescia, Italy

C. Jommi
Politecnico di Milano, Milano, Italy

G. Mayerle
Magistrato alle Acque, Venezia, Italy

ABSTRACT: In the framework of the Mo.S.E. (Electro-mechanical Experimental Module) project for the safeguard of the city of Venezia, an 8.7 m deep basin is being used in the provisional stage for gate caissons precasting. The basin perimeter embankment is delimited by a cofferdam realised by sheet piling on the sea side, and by a CSM (Cutter Soil Mixing) diaphragm wall on the land side. Dewatering operations lasted about 5 months to reach the steady state regime, and they affected the silty foundation deposits which were partially desaturated. The results of FEM numerical analyses of the dewatering operations are presented, focusing on the hydraulic regime and groundwater control. A non-linear analysis was performed, accounting for desaturation of the upper deposit layers, promoted by the dewatering operations. Parametric analyses were run to analyse the effects of hydraulic conductivities ratios and of their absolute values on the dewatering operations. The comparison between recorded data and numerical results allowed for the determination of the large scale hydraulic conductivities of the Venetian deposits, and showed the role played by anisotropy and possible non homogeneous permeability of the barriers on the performance of the cofferdam.

1 INTRODUCTION

The historical city of Venice is one of the most known and famous Italian site worldwide, especially for its unique correlation between land and water. The life of the city depends on the preservation of this delicate equilibrium between the ground level and the sea level.

Today, as in the past, high tides periodically submerge the town, causing serious damages to buildings and activities. In the last century, the frequency of over 110 cm tides has dramatically increased from 2 to 50 events in 10 years. For this reason, in the ’70s, the Italian Government initiated an experimental programme for the safeguard of Venice and of its Lagoon. In 1989 the project proposed by the Consorzio Venezia Nuova for the control of tidal flow into the Lagoon was approved, consisting in the construction of mobile barriers at the three Venetian Lagoon inlets of Lido, Malamocco and Chioggia. These barriers, named Mo.S.E., will separate temporarily the lagoon from the sea in case of high tides, yet guaranteeing the continuity of the marine traffic inward and outward the Lagoon.

To this purpose, a widespread geological and geotechnical study was carried out. Standard and non-conventional laboratory and field tests were performed, for the description of the stratigraphic profiles and the characterisation of the Venetian soils.

Figure 1. Harbour construction: (a) before and (b) after dewatering operations.

The works for the Mo.S.E. started in 2003, and they are proceeding in parallel at the inlets of Lido, Malamocco and Chioggia. In the framework of the Mo.S.E. project, a harbour basin was constructed (Fig.1a). After dewatering (Fig.1b), the basin is being used in the provisional stage for gate caissons precasting at the inlet of Lido-Treporti. During the dewatering operations water discharge was measured at the well points, and water pressure in different borings was recorded to verify the variations of the piezometric level in the area affected by pumping. Dewatering was back analysed numerically with a finite element approach. The parameters of the model were given initially the design values. Afterwards, they were modified with the aim of reproducing the piezometric head profiles with distance from the basin, and the inflow into the wells measured when stationary conditions were reached. The results of the numerical analyses are presented and discussed in the following.

2 THE LIDO-TREPORTI HARBOUR

Lido is the northern and largest of the three lagoon inlets, where the sea bed is encountered at varying depth. Two gates at Lido inlet, namely one at Lido-Treporti and the other at San Nicolò, were designed to overcome the different seabed depth. At the centre of the inlet, a new artificial island is being realised, which will act as the intermediate structure between the two rows of mobile gates.

The coast on the north side of the inlet (Cavallino-Treporti) has been extended and redesigned with the construction of two small harbours, one on the sea side and one on the lagoon side, linked by a lock to allow crafts to shelter and transit when the gates are raised during a high water event. Since the realisation of the gate caissons for the barrier foundation needs a very wide area, in the provisional stage, the 100x450 m floor of the seaside basin is being used for precasting the gate caissons.

To this purpose, a system of embankments was designed and constructed along the basin perimeter. Waterproofing was achieved by a deep cut-off barrier realised by sheet piling on the sea side, and by a CSM diaphragm wall on the land side, to reach a depth of 25 m under the sea level. Bentonite and cement slurry (b/w=0.06, w/c=2.0) was injected during both penetration and retraction. Soil was mixed with 300 kg/m^3 of cement. Dewatering operations required about 5 months, and they were performed by means of a system of wells, realised along the internal perimeter of the embankments (Fig. 2). The phreatic surface inside the basin was lowered down to -19. m under the sea level in the wells. The water discharge was continuously monitored, together with the piezometric level inside and outside the basin, up to 500 m far from the excavation.

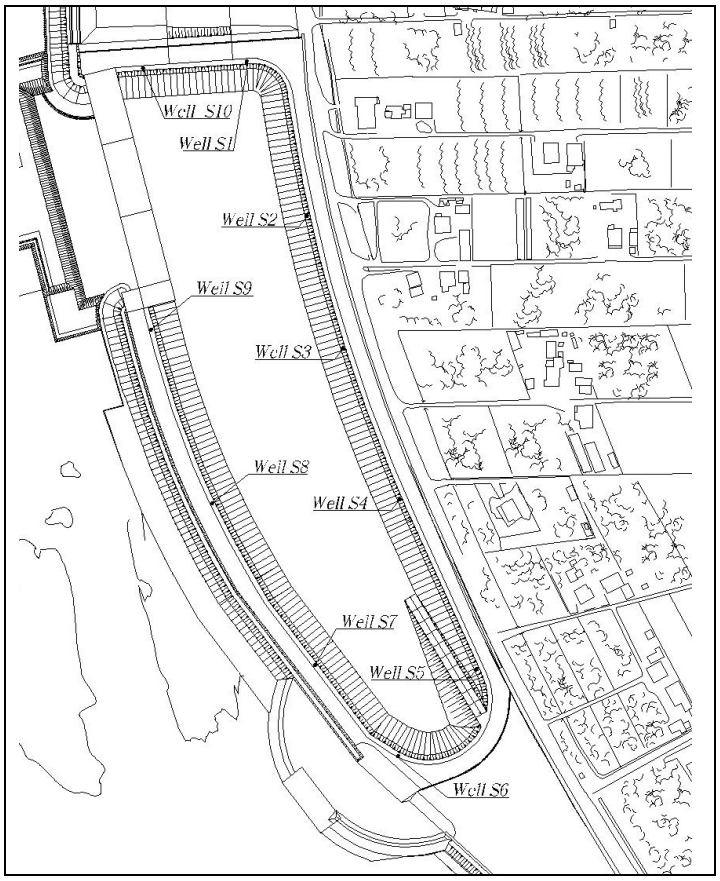

Figure 2. Harbour plan with the well points.

3 GEOTECHNICAL MODEL

The Venice Lagoon originated during the last Flandrian transgression, about 6000 years ago, when the sea level increased and the pre-existing lacustrine basin was filled by the sea water. Its deposits are due to complex alternation of fluvial and marine sediments, depending on the current relative level of the sea with respect to the land in the depositional time period. Nonetheless, all the sediments of Venezia present similar mineralogical composition, due to their common geological origin and similar depositional environment (Belloni at al. 2007).

3.1 *Soil profile and soil classification*

The soil profile shows a complex inter-bedding of layers with a common predominant silty fraction, with different percentages of clay and sand. The 95% of the soils can be classified as medium-fine sands (SP-SM) or silts (ML) and very silty clays (CL). The natural water content ranges between 20% and 30% throughout the depth. Liquid limit is in the range 30-40%, while plastic limit is about 20-30%.

A rough scheme of the Treporti soil profile is presented in Figure 3, together with a section of the basin excavation and of the cofferdam. Five different layers may be identified. The upper layer (A) is essentially composed by medium-fine sand, down to the top of the Caranto at about 13 m depth. The Ca-

ranto, a very silty clay layer, overconsolidated due to ageing and desiccation, belongs to the second depositional layer (B) that is mostly composed by slightly overconsolidated silty clays. The third layer (C) is characterised by a predominant sand fraction, and it overlies a predominantly cohesive formation (D), where the cofferdam is embedded. The last stratigraphic level considered in the model is a sandy layer (E), which is followed by a silty clay layer, starting at 80 m under the sea level, which was assumed as the geometric lower boundary of the numerical model.

3.2 *Hydraulic characterisation*

The hydraulic conductivity had been investigated before the beginning of the operations by means of both laboratory and in situ tests. Oedometer tests gave values in the range $k^{sat} = 10^{-8} \div 10^{-9}$ m/s for the silty and clayey layers. As for the more permeable layers, constant head permeability tests were performed in the triaxial cell on specimens from the upper sand layer (A). Lefranc tests were performed in the more permeable layers at various depths. The results of the laboratory and the in situ tests are compared in Figure 4, as a function of mean effective stress. As expected, the values determined in situ are generally higher than those determined in the laboratory for the same layer.

The dewatering operations at the Lido-Treporti site involved desaturation of an extended area over the lowered water table. To account for reduced hydraulic conductivity of the unsaturated upper layers and to allow accounting for the contribution of these layers to water discharge, a model for the hydraulic unsaturated behaviour was adopted.

In the absence of direct experimental data collected in the specific site, the water retention curves

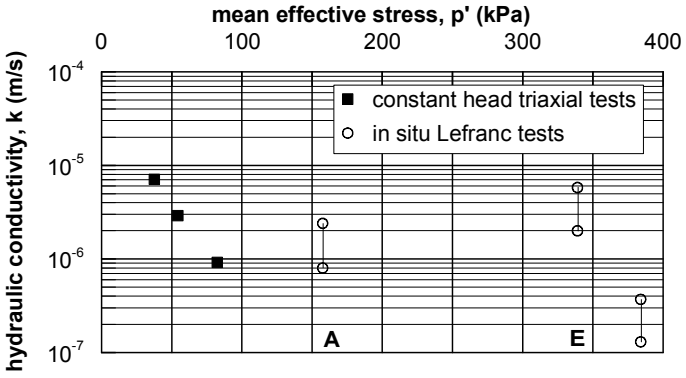

Figure 4. Hydraulic conductivity of the sandy layers from laboratory and in situ tests.

and the relative hydraulic conductivities of the relevant layers were estimated, based on previous studies on similar silty soils (Caruso & Jommi 2005, Cola et al. 2005).

As only monotonic desaturation paths were of interest, a standard van Genuchten (1980) relationship was adopted to model the drying branch of the water retention curve,

$$S_r = \left(1 + \left(\frac{s}{P}\right)^{\frac{1}{1-r}}\right)^{-r} , \qquad (1)$$

relating the degree of saturation S_r to the suction, s, identified with the difference between atmospheric air pressure and water pressure. The parameters $P = 0.01$ MPa, $r = 0.11$, and $P = 0.05$ MPa, $r = 0.12$ were assumed for the coarser and finer soil layers, respectively.

The hydraulic conductivity was assumed to decrease with saturation degree from its saturated value, through a multiplicative relative permeability coefficient k_{rel}, which was given the power law $k_{rel} = S_r^5$.

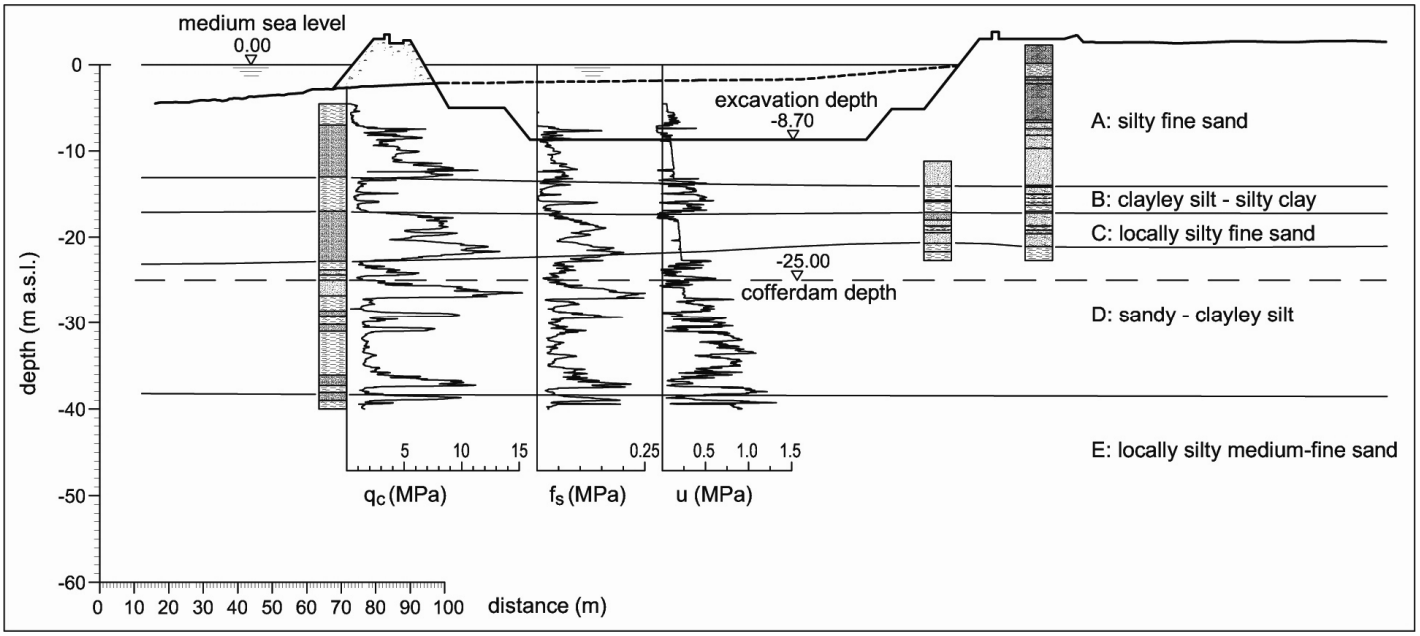

Figure 3. Lido-Treporti stratigraphic profile.

4 NUMERICAL MODEL

Non linear, 2-D, numerical simulations were run to back-analyse the hydraulic characteristics of the lagoon soil layers at the large scale involved in the dewatering operations. Displacements and pore pressure fields were analysed, though with an uncoupled procedure. Only the results of the hydraulic problem will be presented in the following. The analyses were run with the FEM code Abaqus 6.7.

Assuming constant water density, and given the porosity, the differential equation governing the water mass balance simply reads:

$$\nabla^{\mathrm{T}} \left(\mathbf{k} k_{rel} \nabla h_w \right) = n \frac{\partial S_r}{\partial t} , \tag{2}$$

where h is the hydraulic head, $\mathbf{k}$ is the hydraulic conductivity tensor, with reference to saturated conditions, k_{rel} is the relative permeability coefficient, n is the porosity, and S_r is the degree of saturation.

A standard Galerkin FE approximation was adopted in the discretisation. The 2D model of the cross section of the basin (between wells *S3* and *S8* in Fig. 2) covers the 1200 m wide and 80 m deep area represented in Fig. 5. The mesh is composed of 19661 triangular elements (39865 nodes), with quadratic interpolation of hydraulic head. Notable refinement was provided close to the wells and the cofferdam, where high pressure gradients develop.

To assure a stable numerical solution for the transient hydraulic problem the numerical time step must satisfy the following inequality

$$\Delta t > \frac{n \gamma_w}{6 k(S_r)} (\Delta l)^2 \frac{dS_r}{ds} , \tag{3}$$

where γ_w is the water specific weight, $k(S_r)$ is the current value of the hydraulic conductivity, dS_r/ds is the storage coefficient, calculated from the retention curve, and Δl is the characteristic dimension of a finite element. Although a very fine mesh was adopted where desaturation could occur, the smaller elements had a typical dimension of about 1. m. Given the soil layers hydraulic conductivity, the minimum time step required to guarantee the stability of the numerical solution is $\Delta t \approx 1$ month, which results comparable to the time required to complete the dewatering operations. For this reason, it was decided to proceed with a series of steady state analyses, instead of solving the fully transient problem.

With reference to Figure 5, the average sea level was imposed on the boundary AB, while the lower boundary BC, corresponding to the top of a deep cohesive layer, was assumed impermeable. On the land side lateral border of the model, CD, located about 500 m far from the cofferdam, the hydraulic head resulting from piezometer readings was imposed. Preliminary parametric analyses were performed to limit the influence of the mesh discretisation on the numerical results (Cividini & Gioda, 2007).

On the upper boundaries DE and AF, exposed to the atmosphere, a non-linear condition, allowing for incoming flow only for positive water pressure, was imposed throughout the whole analysis. On the basin perimeter EF, the boundary conditions were progressively changed throughout the dewatering stages. The hydraulic head was lowered, consistently with the field data, followed by the introduction of the same non-linear condition described previously.

To simulate the dewatering process, the piezometric heads recorded at the internal wells during dewatering were imposed to the boundary of the numerical wells (WP_S, WP_L in Fig. 5).

Hydraulic conductivities of the relevant layers and of the cofferdam elements were given initially the isotropic design values (T) reported in Table 1. Afterwards, parametric analyses were performed, by changing the hydraulic conductivity of the coarser layers and of the diaphragm wall, and introducing different anisotropic ratios for the soil layers. Table 1 summarises the input values adopted in the analyses (horizontal conductivities and vertical to horizontal conductivity ratios) which will be discussed in the following, focusing on the final hydraulic steady state regime at the end of dewatering operations.

Table 1. Horizontal hydraulic conductivities k_H (m/s), and anisotropy ratios (k_V / k_H) for the soil deposits: design values (T) and numerical values (sets A, B, C).

Materials	T	A	B5	B10	C5	C10
Coarse grain deposits	10^{-6}	10^{-5}	10^{-5}		10^{-5}	
Fine grain deposits	10^{-8}	10^{-8}	10^{-8}		10^{-8}	
Sheet pile	10^{-12}	10^{-12}	10^{-12}		10^{-12}	
Diaphragm wall	10^{-9}	10^{-9}	10^{-10}		10^{-10}/4x10^{-9}	
Ratio k_V/k_H	1	1	0.2	0.1	0.2	0.1

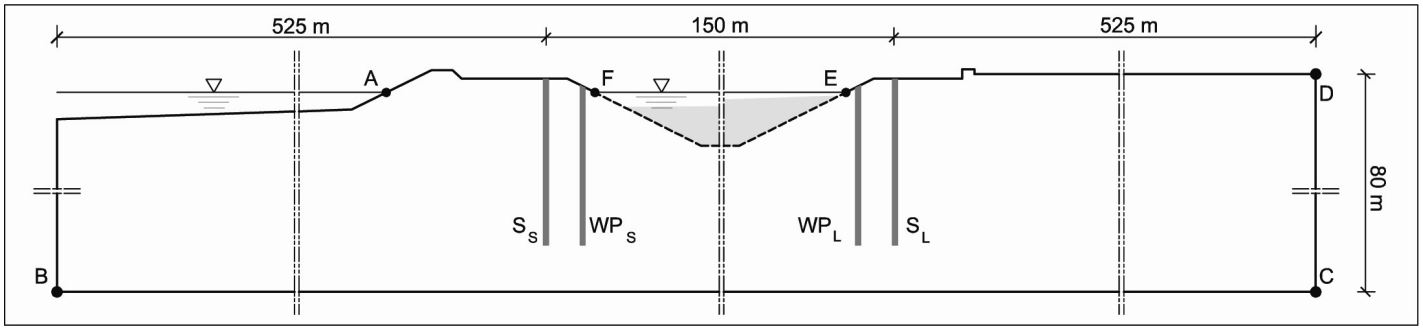

Figure 5. Geometrical model of the problem.

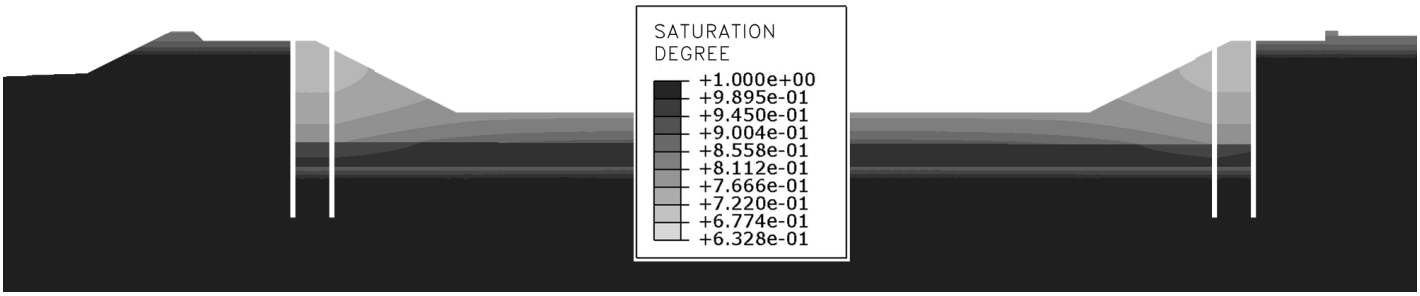

Figure 6. Contours of the degree of saturation: results of analysis B10.

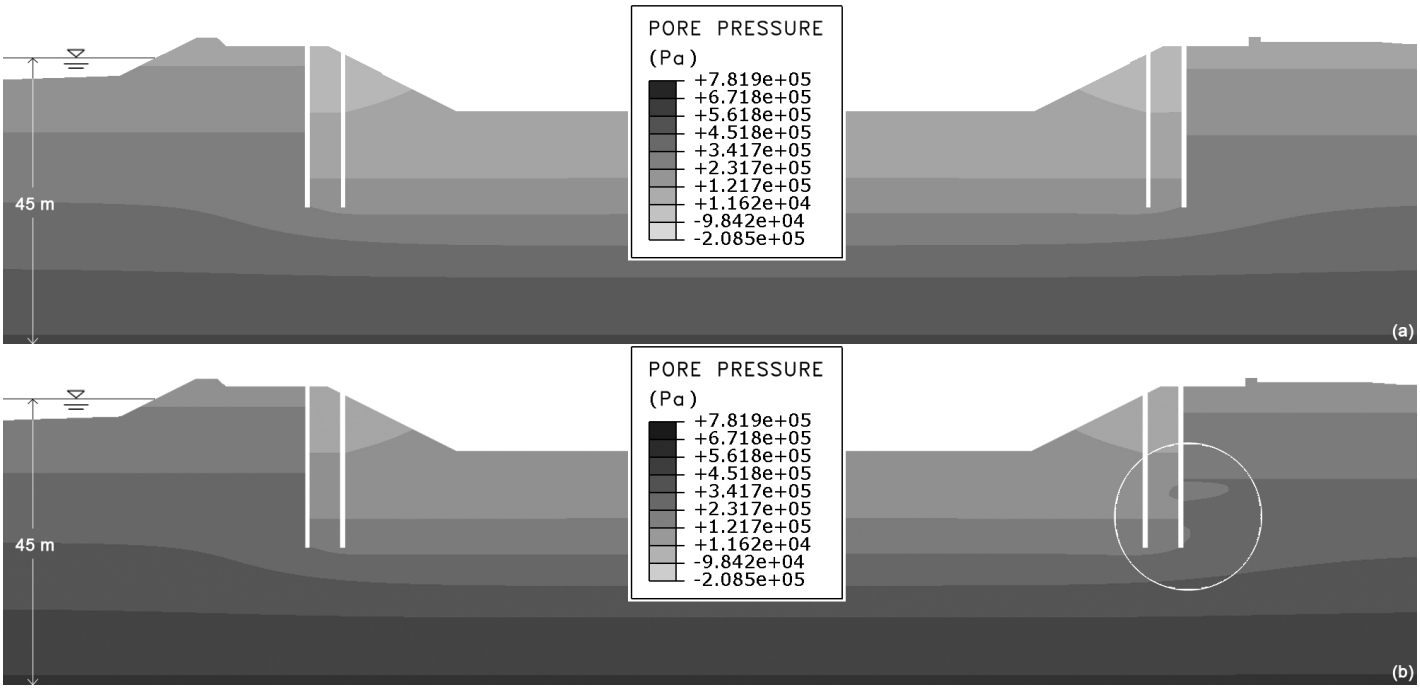

Figure 7. Contours of the pore pressure distribution results of the analyses (a) B10, and (b) C10.

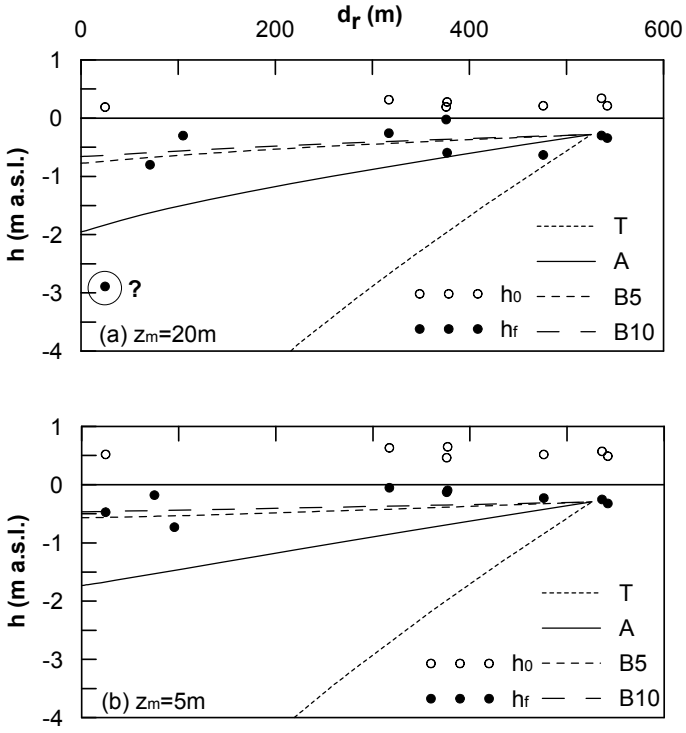

Figure 8. Piezometric profile on the land side: comparison between initial (h_0) and final steady state (h_f) field data and calculated values from analyses T, A, B5, B10.

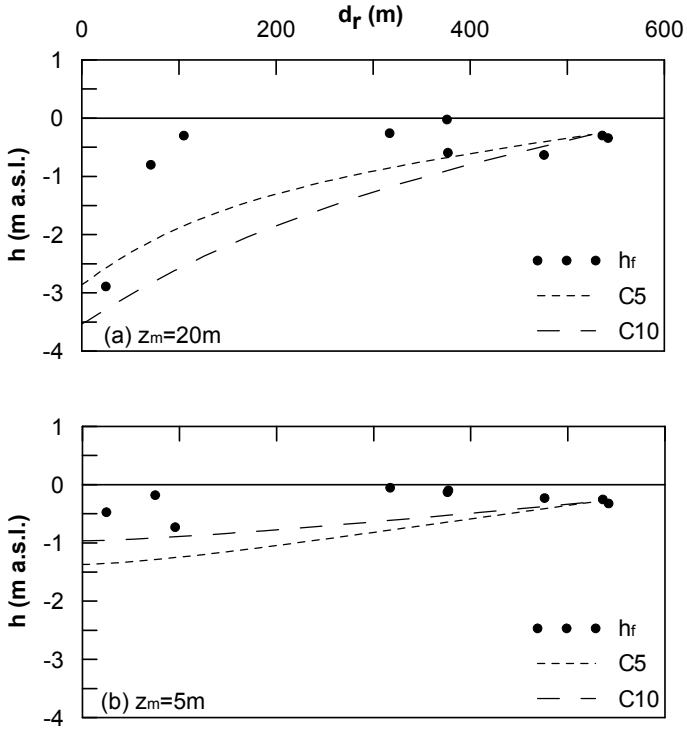

Figure 9. Piezometric profile on the land side: comparison between field data at steady state and calculated values from analyses C5 and C10.

5 DISCUSSION OF THE RESULTS

Typical contours of the degree of saturation are depicted in Figure 6. Desaturation occurs in coarser layers, while the intermediate layers remain almost saturated, except a limited zone near to the well. The groundwater regime is affected only close to the basin down to a depth of about -35. m under the sea level (Fig. 7). The measured piezometric heads recorded on the land side at the beginning and the end of dewatering are reported in Fig. 8, with open and filled symbols, respectively, as a function of their radial distance, d_r, from the basin perimeter. Scatter is mostly due to their different alignment with respect to the cross section examined. The data show that the piezometric head decreases both near to the surface (Fig. 8a) and at depth (Fig. 8b) of about -1 m with respect to its initial value.

As the piezometric profile is governed by the relative hydraulic conductivities ratios of the different elements (soil layers, sheet-pile and diaphragm), a parametric back-analysis allowed for determining the ratios necessary to describe the data recorded. To catch the correct orders of magnitude of the hydraulic conductivities, comparison was made with the volume of water drained from the well system. The comparison between the measured discharge per unit length and the ones calculated from the different analyses is reported in Figure 10. The numerical analyses showed that:

– the water discharge is substantially underestimated if reference is made to the design conductivity values, calibrated on the laboratory and in situ tests;

– if the hydraulic conductivity of the coarser layers is increased by one order of magnitude, better results are obtained, although water discharge is slightly overestimated and the piezometric heads are still lower than those recorded;

– the data seem to suggest that the diaphragm wall on the land side has an average lower hydraulic conductivity than expected, being better represented by a value which is an order magnitude less than that assumed in the preliminary design stage;

– only an anisotropic hydraulic conductivity tensor may justify the recorded piezometric profile, and catches quite well the recorded water discharge.

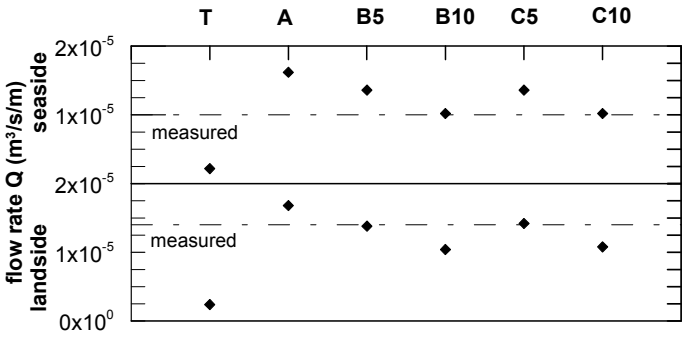

Figure 10. Measured and calculated flow rates on the sea side and on the land side.

Two vertical to horizontal permeability ratios were investigated, namely k_V / k_H = 1/5, 1/10. The two ratios do not change significantly the piezometric profile, but affect slightly the water discharge. Best fit is obtained with a ratio of 1/5 on the landside and with an increased ratio of 1/10 on the seaside.

To try to justify the low hydraulic head recorded just behind the diaphragm wall in one of the wells, it was assumed tentatively a locally non homogeneous hydraulic conductivity of the diaphragm wall (analysis C). The results of the analysis show that the consequent localised decrease in pore pressure, evidenced in Figure 7b, does not affect much the total water discharge (see Fig. 10), but may justify the low hydraulic head recorded at depth behind the diaphragm (Fig. 9a) in a single location.

6 CONCLUSIONS

The results of the numerical analyses, compared to the data recorded during and after dewatering, allowed for the determination of the large scale hydraulic conductivities of the Venetian Lagoon soil layers. With respect to the initial design values, the coarser layers had to be given a higher hydraulic conductivity in the horizontal direction to catch correctly both the piezometric profile and the amount of pumped water, highlighting the role played by anisotropic hydraulic conductivity on the piezometric head distribution. Local non homogeneous hydraulic conductivity of the CSM diaphragm may explain anomalous data recorded in the field, but does not affect substantially the cofferdam response.

AKNOWLEDGEMENTS

The authors gratefully acknowledge the support of the Magistrato alle Acque, the Consorzio Venezia Nuova and the Technital S.p.A..

REFERENCES

Belloni, L.G., Rizzo, A., Caielli, A. & Mayerle, G. 2007. Influenza sedimentologica sulle caratteristiche geotecniche dei terreni della Laguna Veneta. *XXIII Convegno Nazionale di Geotecnica*, Padova, Patron Editore: 147-159.

Caruso, M. & Jommi, C. 2005. An evaluation of indirect methods for the estimation of hydraulic properties of unsaturated soils. *Problematic Soils*, Bilsen H. & Nalbatonglu Z. (eds.), Eastern Mediterranean University Press 1: 183–191.

Cividini, A. & Gioda, G. 2007. Back-analysis approach for the design of drainage systems. *Int. J. of Geomech.*, 7: 325-332.

Cola, S., Simonini, P. & Sanavia, L. 2005. Modelling pore pressure response as a function of tide in the Venice Lagoon marshes. *Proc. 11th IACMAG*,.3: 101-108.

van Genuchten, M. 1980. A closed form equation for predicting the hydraulic conductivity of unsaturated soils. *Soil. Sci. Am. J.*, 44: 892-89.